

AFOSR 68-0231

AD664602

GRANT AF EOAR 67-09

30 November 1967

FINAL SCIENTIFIC REPORT

LAMINAR SEPARATION IN HYPERSONIC FLOWS

1 October 1966 - 30 September 1967

JEAN J. GINOX

von Karman Institute for Fluid Dynamics
Rhode-Saint-Genèse, Belgium

CR 67-G4-I-1

DDC
RECEIVED
FEB 2 1968
RECEIVED
C

This document has been approved for public
release and sale; its distribution is unlimited

This research has been sponsored in part by the Air
Force Office of Scientific Research, through the European Office
of Aerospace Research, OAR, United States Air Force, under Grant
AF EOAR 67-09.

Reproduced by the
CLEARINGHOUSE
for Federal Scientific & Technical
Information Springfield Va. 22151

Distribution of this
document is unlimited

GRANT AF EOAR 67-09

30 November 1967

FINAL SCIENTIFIC REPORT

LAMINAR SEPARATION IN HYPERSONIC FLOWS

1 October 1966 - 30 September 1967

JEAN J. GINOUX

von Karman Institute for Fluid Dynamics
Rhode-Saint-Genèse, Belgium

CR 67-G1-I-1

This document has been approved for public
release and sale; its distribution is unlimited

This research has been sponsored in part by the Air
Force Office of Scientific Research, through the European Office
of Aerospace Research, OAR, United States Air Force, under Grant
AF EOAR 67-09.

Summary

An experimental investigation of the laminar flow over a cone-cavity model with a rounded reattachment shoulder at zero angle of attack was conducted at $M = 5.4$. For mass injection into the cavity at rates up to eight-tenths the boundary layer mass flow at separation, the pressure and heat transfer distributions along the surface were obtained, with emphasis on the reattachment zone. A simple empirical correlation was established between reattachment pressure and heat transfer peaks as a function of injection rate.

1. Introduction

For a number of years, it has been known that the presence of a cavity in the surface on a hypersonic body gives rise to a significant redistribution of surface pressure and heat transfer to the body (ref. 1, 2, 3). Specifically, these quantities are reduced in the region of separated flow, but experience a sharp increase within the vicinity of reattachment, followed by a decrease toward the undisturbed values in the downstream area. In many practical applications, the primary undesirable feature of this phenomenon is the elevated pressure and heat transfer at reattachment. This fact justifies further research into methods of substantially reducing these peak values.

In this regard, it has been previously theoretically predicted and experimentally verified that injection of a small amount of gas into the separated region accomplishes this result (ref. 1, 4, 5, 6). There is, however, very little detailed experimental pressure and heat transfer data available describing these distributions in the reattachment region for injection rates of interest. In fact, a recent attempt to formulate a semi-empirical description of the pressure and heat transfer rise for the more elementary case of zero injection has focused attention upon this deficiency (ref. 7). The present research effort was initiated in response to this need.

This investigation was directed toward provision of detailed static pressure and heat transfer distributions (more detailed than in the preliminary study of ref. 6), over the entire surface of a cone-cavity model, and particularly in the reattachment region, by using cavities with rounded reattachment shoulders, as opposed to NICOLL's ones which had 90° sharp corners. One objective of the research was to provide an empirical correlation between pressure and heat transfer distributions.

The pressure and heat transfer studies were carried out in parallel, respectively by E. CALLENS, Jr. and J. KENNEDY, in partial fulfillment of the requirements for the diploma of the von Karman Institute for Fluid Dynamics, under the supervision of the author, principal investigator. The results of these two investigations will be reported in detail (ref. 8, 9) and will only be summarized in the present final scientific report.

2. Experimental equipment

2.1 Wind tunnel

All experiments were conducted in the VKI hypersonic wind tunnel H-1 at a Mach number of 5.4. The size of the test section is $12 \times 12 \text{ cm}^2$, giving a uniform flow with $\pm 1/2$ per cent variation in Mach number. The stagnation temperature was about 250°C . The stagnation pressure was of 15 atms. for the pressure measurements and 16 or 31 atms. for the heat transfer studies, corresponding to free stream Reynolds numbers of 1.3×10^5 or 2.5×10^5 per centimeter, respectively.

2.2. Models

The basic model configuration was a 10° semi-apex angle cone incorporating an annular cavity of the short-deep type. The cavity was 12 mm wide and 4 mm deep. It was located 42 mm downstream of the sharp nose of the model.* The injected gas (air) entered the cavity tangentially to the floor from an annular port (1 mm wide) located at the base of the reattachment shoulder, which had a 4 mm radius. The separation shoulder was a sharp 90° turn.

* on the heat transfer model. 37.5 mm on the pressure model.

Separate models were instrumented and used for the static pressure and heat transfer measurements. They are fully described in refs. 8 and 9. The detailed determination of reattachment pressure and heat transfer rises required that several sensors (pressure taps or thermocouples) be located within a distance of 6 millimeters in the vicinity of reattachment. In order to do so, they had to be staggered.

The pressure model used in ref. 8 was designed with 0.3mm inner diameter tubing which gave rather large response times. As some doubt arose about the existence of a second pressure peak observed downstream of reattachment, a second model was redesigned with 0.45mm inner diameter tubing, which gave better performance and which did not show a second pressure peak. Except when specified, the results presented in this report were obtained on the latter model.

Heat transfer rates were measured by the thin-skin techniques. Attempts to produce chemically or electrolytically plated nickel models, with very small skin thickness (i.e. 0.3mm), were unsuccessful during the reporting period. The results described in this report are related to stainless steel model CHT-2 of ref. 9, which had a skin thickness of 0.8mm and copper constantan thermocouple wires of 0.06 and 0.01mm diameter. This model was less instrumented than hoped and thermocouples were not staggered. Temperature-time histories were measured on CEC galvanometric recorders and heat transfer coefficients computed assuming a constant value of the recovery temperature equal to the theoretical cone value.

2.3 Injection plant

An injection plant was designed to supply a precise amount of

clean, dry air to the plenum chamber of the cavity models. The air was supplied to the model at room temperature (about 20°C) and entered the cavity at a temperature nearly equal to the external wall temperature of the model (about 50 to 100°C for the pressure model exposed to long running times and about 20°C for the heat transfer model tested with shorter running times.

In this report, the injection rate is normalized with the theoretical mass flow rate (Q_{BL}) in the boundary layer at separation

$$C_q = Q_{inj}/Q_{BL}$$

Q_{BL} was equal to 20.5 liters/minute based on standard atmospheric conditions for stagnation conditions of 210°C and 15 atms. (assuming a wall temperature of 100°C) and 25.5 liters/minute at 210°C and 16 atms., based on a wall temperature of 20 °C. C_q was varied in the tests in steps over a range of zero to 0.84 maximum.

A particular injection rate of interest is that required to reduce the heat transfer within the cavity to zero, as theoretically predicted by CHAPMAN (ref. 1). Referred to as "Chapman's value" in this report, this injection rate was calculated to be 28 percent of Q_{BL} for the pressure model and 20 percent for the heat transfer model at a stagnation pressure of 16 atms.

2.4 Flow visualization

Schlieren and shadow pictures of the flow around the cone-cavity model were taken at each injection rate that was used. The steadiness of the flow was verified from high speed motion pictures (3000 frames/sec.).

In addition, surface flow visualization was made by dyeing the model surface with blue steel ink and then coating it with a viscous white mixture of bioxide of titane, talc, oil and kerosense. A sublimation technique was also employed, using acenaphthene as the subliming agent.

2.5 Overall precision

It is estimated that the pressure distributions obtained in this study are accurate to ± 3 percent in the reattachment zone. This was carefully examined in great detail in ref. 8 after considering the effects of: tunnel variations, model incidence and yaw, temperature variations, pressure response time, uniformity of injection, instrument error and calibration, control parameters variation, flow steadiness, model design features such as tap location and nose-afterbody alignment, data reduction.

A larger uncertainty existed in the heat transfer data, partly due to random variations of the stagnation temperature, following an initial unexplained overshoot of this temperature. Uncertainty about the exact model skin thickness is also included in the results. Finally, no correction was made for transverse heat conduction through the model skin and heat losses along the thermocouple wires. It is estimated that the heat transfer data is accurate to ± 5 to 10 percent.

3. Results and Discussion

3.1 Flow visualization

Schlieren and shadow photographs of the flow over the cavity model are presented in ref. 8 for various injection rates. They show the following results :

At $C_q = 0$ (no injection), an expansion fan existed at separation and a shock appeared at reattachment, in agreement with the pressure data. For increasing injection rate, the separation expansion and reattachment shock both diminish in intensity. Near $C_q = 0.18$, the separation expansion completely disappears. The reattachment shock becomes very weak but never disappears. It moves slightly forward for higher injection rates and is seen to be rooted in the free shear layer for $C_q = 0.7$. This movement corresponds to the upstream displacement of the maximum pressure. A separation shock appears at $C_q = 0.21$ and becomes stronger with additional injection.

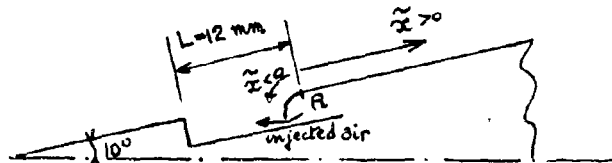
At $C_q = 0$, the flow is laminar over most of the body surface. Transition moves forward with injection until it is about one cavity length downstream of reattachment at $C_q = 0.7$. The nearness of transition to reattachment may explain, in part, the radical changes in afterbody pressure and heat transfer distributions that were observed for the highest injection rates. The separated boundary layer is clearly lifted from the surface at reattachment and converges back toward the surface downstream of this region.

Combined effects of surface shear stress and elevated temperature at reattachment were revealed in the sublimation photographs at $C_q = 0$. The sublimation rate was extremely large along an annular area located near reattachment. This effect diminished rapidly with mass injection, and, at Chapman's value, no trace of sublimation is seen. An incidental observation from these tests was the appearance of symmetrical longitudinal striations on the afterbody above $C_q = 0.18$.

The surface flow visualization photographs presented in ref. 8 show a distinct line exactly at the location of the reattachment pressure peak. This line remained stationary with injection but decreased in intensity until it was no longer clear at $C_q = 0.18$. It was then concluded that reattachement was located very close to the pressure peak, i.e. about 1 mm upstream of the junction of the reattachment shoulder to the conical afterbody.

3.2 Pressure measurements

Detailed measurements made in the reattachment zone, on the model equipped with 0.45 mm inner diameter pressure tubing, are plotted in figures 1 to 4. In these figures, the measured static pressure is referred to the cone pressure (P_c) measured on the forecone, 20 mm downstream of the nose. L is the cavity width (i.e. 12 mm) and \tilde{x} is the surface distance measured along a model generator with its origin at the junction (R) of the reattachment shoulder and the afterbody, as show in the sketch :



The pressure distribution without mass injection is shown in figure 1. An average curve is drawn through the data points of several runs, each being represented by a different symbol. The pressure variations around the average curve is seen to be of the order of ± 3 percent. Also shown in figure 1, for comparison, is the zero injection pressure distribution of ref. 8, which was obtained on an identical model, but equipped with smaller pressure taps.

From this figure, a number of observations can be made which illustrate the character of the flow phenomena involved. First, the cavity floor pressure is 10 percent below cone pressure, this being in good agreement with the results of NICOLL (ref. 4) for a cavity of similar length to depth ratio and a similar unit Reynolds number. In addition, the pressures at two cavity floor stations never differed by more than 1/3 percent, thus verifying NICOLL'S conclusions that the floor pressure is virtually constant for this type of short-deep cavity.

The pressure rise is linear over a large portion of the compression zone, being non-linear only during the initial rise and near the peak value. This fact is useful in extrapolating less detailed measurements of other investigators. The peak pressure is 1.53 times cone pressure and 1.7 times cavity floor pressure. As shown in ref. 8, the efficiency of the compression process was about 50 percent.

The pressure on the afterbody decreased continuously with distance downstream of the pressure peak falling below cone pressure at an \tilde{x}/L of about one.

Similar trends were observed in the earlier measurements of ref. 8, except for the existence of a second small pressure peak in the decaying portion of the pressure distribution, which seems to be explained by the rather large response time of the smaller pressure taps. This is, however, rather intriguing since the heat transfer data, presented in the next section, seems to indicate an oscillatory decay of the heating rate with distance downstream of the peak value.

Figures 2 and 3 show the pressure distributions for different rates of mass injection into the cavity. For clarity of the presentation,

only average curves are shown, the pressure variations being always less than ± 3 percent of the average values. A cross plot of these figures is given in figure 4, where the variation of peak pressure ratio (P_R/P_C) is shown as a function of C_q .

It is seen that mass injection has the effect of reducing the pressure rise in the reattachment region of the flow, while the cavity pressure increases to finally become larger than cone pressure. The reattachment pressure peak decreases sharply and linearly with injection up to about $C_p = 0.1$, then decreases more slowly until a region of constant pressure is reached at $C_q = 0.25$. This region extends to $C_q = 0.32$ and is followed by a pressure peak increase with additional injection. The location of pressure peak remains stationary until the minimum peak value is reached. Beyond this, the maximum pressure location moves forward with injection.

In reference 8, it was found that the second small pressure peak existed over the whole range of injection rates and remained at the same location as in the case of zero injection shown in figure 1.

3.3. Heat transfer measurements

Attempts to use chemically plated nickel models of small skin thickness (i.e. about 0.3mm) were unsuccessful because of their brittleness. More successful were the electrolytical plate cone-cavity models. However, the measured heat transfer distributions showed up repeatable oscillations downstream of reattachment which could be explained during the reporting period. As doubt exists about the nature of this oscillatory decay of the heat transfer coefficient, further investigation will have to be carried on. The results described in this report are related to stainless steel model CHT-2 of reference 9, which had a skin thickness of 0.8mm and which was as

fully instrumented as hoped, particularly in the decaying portion of the heat transfer downstream of reattachment. However, the heat transfer distributions are sufficiently accurately measured, in particular the peak values, to allow a precise correlation to be made with the pressure data.

In this report only the measurements made at a tunnel stagnation pressure (p_0) of 16 kg/cm^2 are presented. Very similar results were obtained at $p_0 = 31 \text{ kg/cm}^2$ which are described in ref. 9.

Figure 5 shows the ratio of the measured heat transfer coefficient (h_m) to the theoretical cone value as a function of the distance x along the conical surface (starting from the lip of the injection port) and of \tilde{x}/L which was used in the presentation of the pressure data. Each curve corresponds to a different injection rate C_q ranging from zero to 0.43. Cross plots of figure 5 are given in figures 6 and 7 which show the variation of the cavity $\left(\frac{h_{mc}}{h_t}\right)$ and peak $\left(\frac{h_{mR}}{h_t}\right)$ heat transfer ratios as a function of the mass injection coefficient C_q .

Figure 6 shows that without mass injection the cavity heat transfer coefficient is of only 68% of the attached flow value. It decreases with mass injection down to about 10 percent of h_r at $c_q = 0$. Similarly it is seen from figure 7 that the peak value of the heat transfer is equal to 2.38 times the attached flow value without mass injection. $\frac{h_{mR}}{h_t}$ decreases sharply and linearly with increasing mass injection until Chapman's value ($C_q = 0.2$) is reached above which the heat transfer peak has disappeared as shown in figure 5. Also seen is that the ratio h_m/h_t is below unity over the whole model surface for C_q larger than about 2.0; except near the model base where h_m/h_t increases again as a result of transition from laminar to turbulent upstream when C_q was increased.

Comparison between figures 2 and 5 shows that the pressure and heat transfer peaks have the same location at $\tilde{x}/L = .065$, i.e. 0.8mm upstream of the junction (R) of the reattachment shoulder with the conical afterbody.

3.4. Comparison between the pressure and heat transfer peaks

Both pressure and heat transfer peaks vary linearly with small injection rates up to $C_q = 0.15$ approximately. Furthermore both peaks have the same location. Therefore, these suggest the following approximate correlation

$$\frac{h_{mR}}{ht} = \frac{2.38 - 9.0 C_q}{1.54 - 2.8 C_q} \frac{P_R}{P_c}$$

Using this expression, one can determine as a function of mass injection, the heat transfer peak at reattachment knowing the experimental pressure peak at zero injection, and the pure cone flow conditions.

4. Conclusions

An investigation has been undertaken in the hypersonic H-1 wind tunnel at the von Karman Institute for Fluid Dynamics at a free stream Mach number of 5.41 to determine in detail the static pressure and heat transfer rate on and downstream of the reattachment shoulder of a 10° cone-cavity model with and without mass injection. The results discussed in this report form the basis for the following main conclusions.

1. The pressure along the cavity floor for the type of short-deep cavity employed is constant for zero injection and, furthermore, remains constant along the floor for mass injection rates of over twice Chapman's value. This cavity floor pressure increases monotonically with injection.

2. The heat transfer rate to the cavity floor is only 68 percent of the pure cone value at zero injection and decreases down to 10 percent at an injection rate about equal to Chapman's value.

3. The pressure rises sharply and linearly in the compression portion of the reattachment zone for zero injection to a peak that is 53 percent greater than cone pressure while the heat transfer rate rises to 2.38 times the cone value.

4. There is no injection rate which will entirely eliminate the pressure rise, although the heat transfer coefficient can be lowered below the cone value for injection rates larger than about Chapman's value.

5. The maximum reattachment heat transfer and pressure occur at the same position, independent of the injection rate and both decrease linearly with increasing mass injection, up to $C_q = 0.15$. A result which lead to a simple empirical correlation between pressure and heat transfer reattachment peaks.

REFERENCES

1. CHAPMAN, D.R.: A theoretical analysis of heat transfer in regions of separated flow. NACA TN 3792, 1956.
2. LARSON, H.K.: Heat transfer in separated flow.
J.A.S. Vol 26, pp 731-738, November 1959.
3. NICOLL, K.M.: A study of laminar hypersonic cavity flows.
AIAA Jnl, vol. 2, no. 3, pp 1535-1541, September 64.
4. NICOLL, K.M.: Mass injection in a hypersonic cavity flow.
ARL 65-90, May 1965.
5. NICOLL, K.M.: An experimental investigation of laminar hypersonic cavity flows. Part II: Heat transfer and recovery factor measurements.
ARL 63-73, January 1964.
6. GINOUX, J.J.: Laminar separation in supersonic and hypersonic flows.
Contract AF-EOAR 66-6. Final Report, September 1966.
7. CHANG, P.K.: The reattachment of laminar cavity flow with heat transfer at hypersonic speed. Tech. Report AF OSR 66-0135, April 1966.
8. CALLENS, E.E. & GINOUX, J.J.: Laminar Hypersonic Cavity Flow with Mass Injection. Part I: Pressure measurements.
VKI Project Report 67-181, June 1967.
9. KENNEDY, J.B. & GINOUX, J.J.: Laminar hypersonic cavity flow with mass injection. Part II: Heat transfer measurements
VKI Project Report 67-186, July 1967.

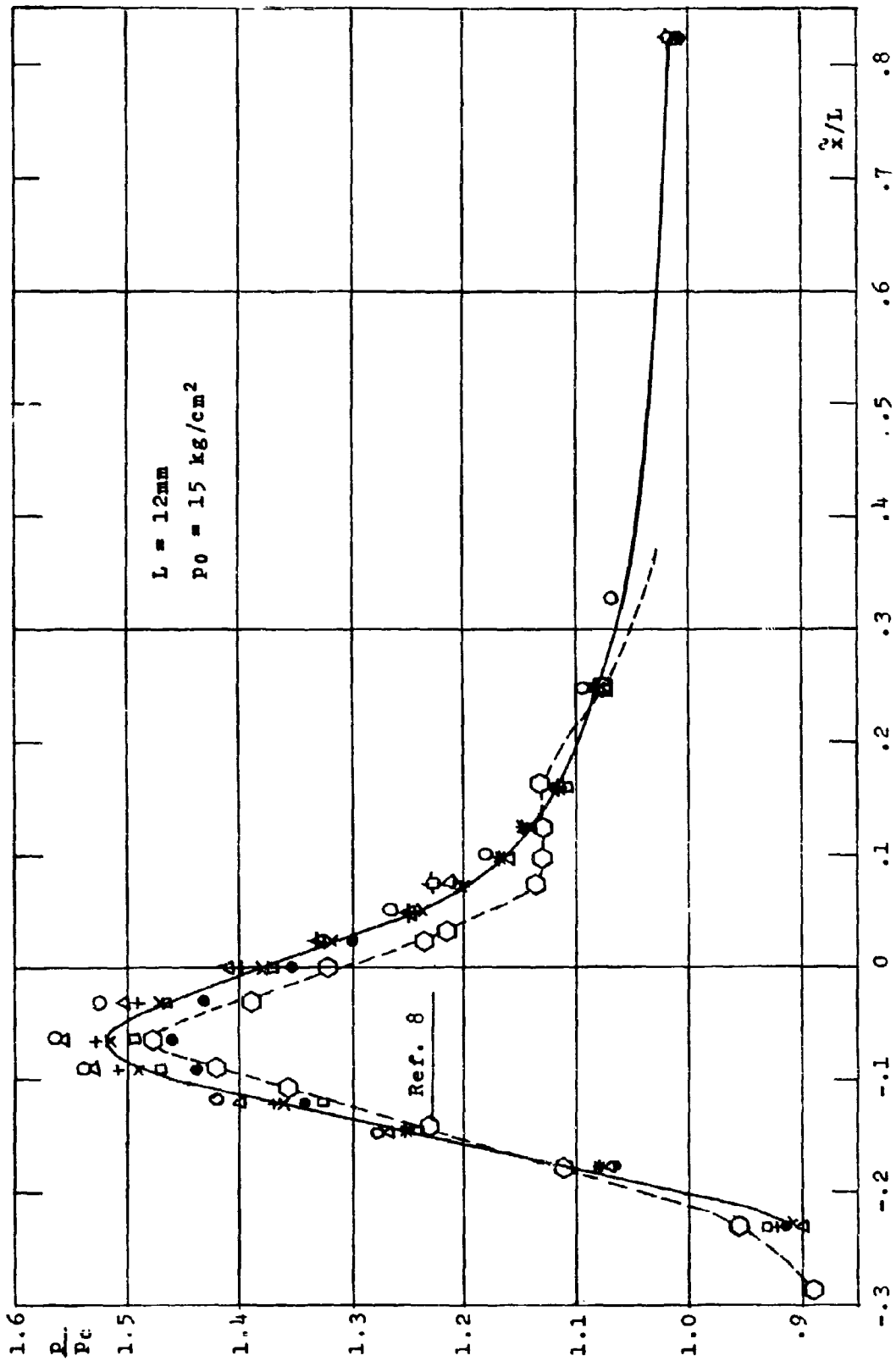


Figure 1. Pressure distributions on cone cavity model at $C_q = 0$

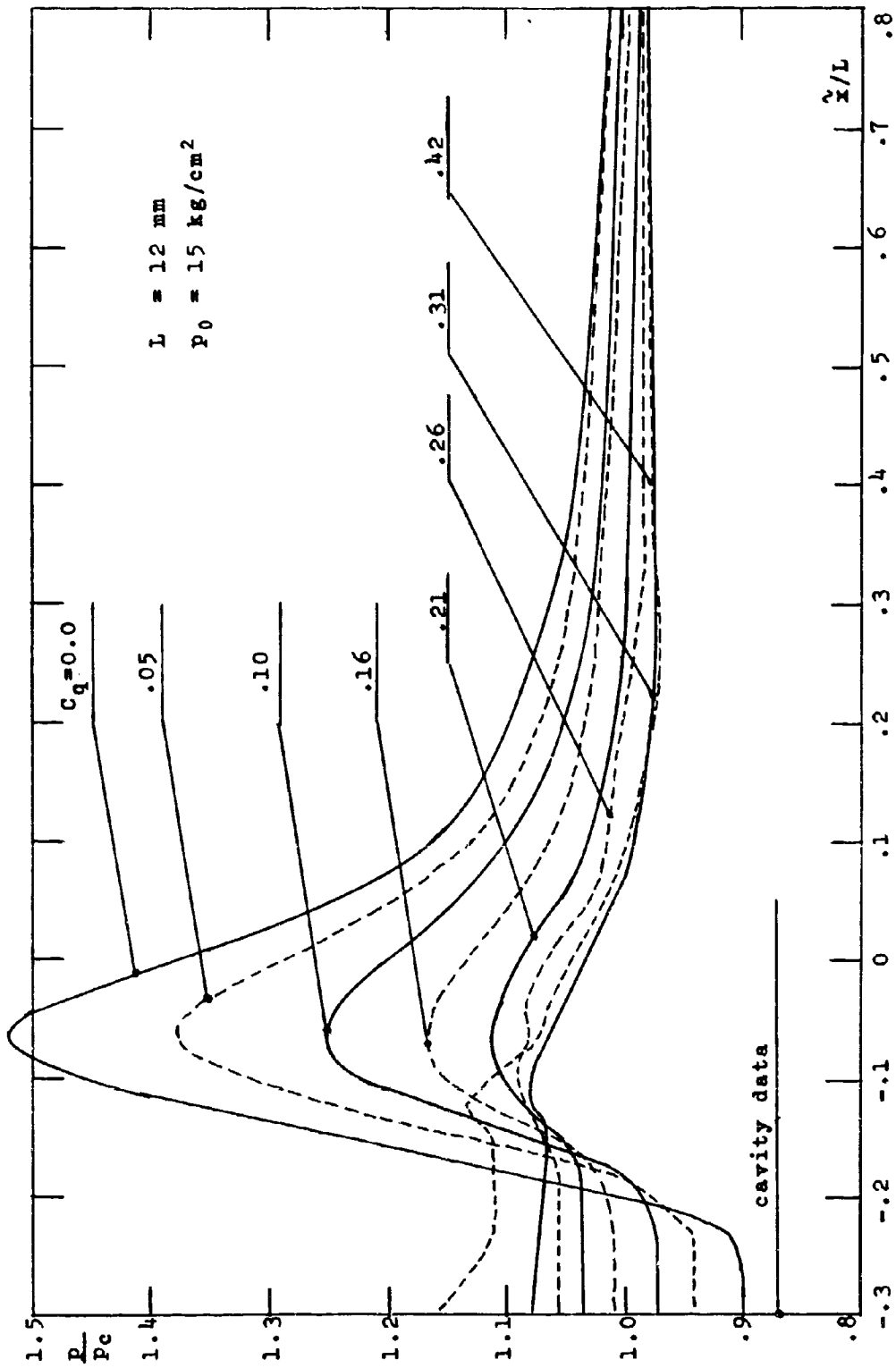


Figure 2. Effect of mass injection on the pressure distributions

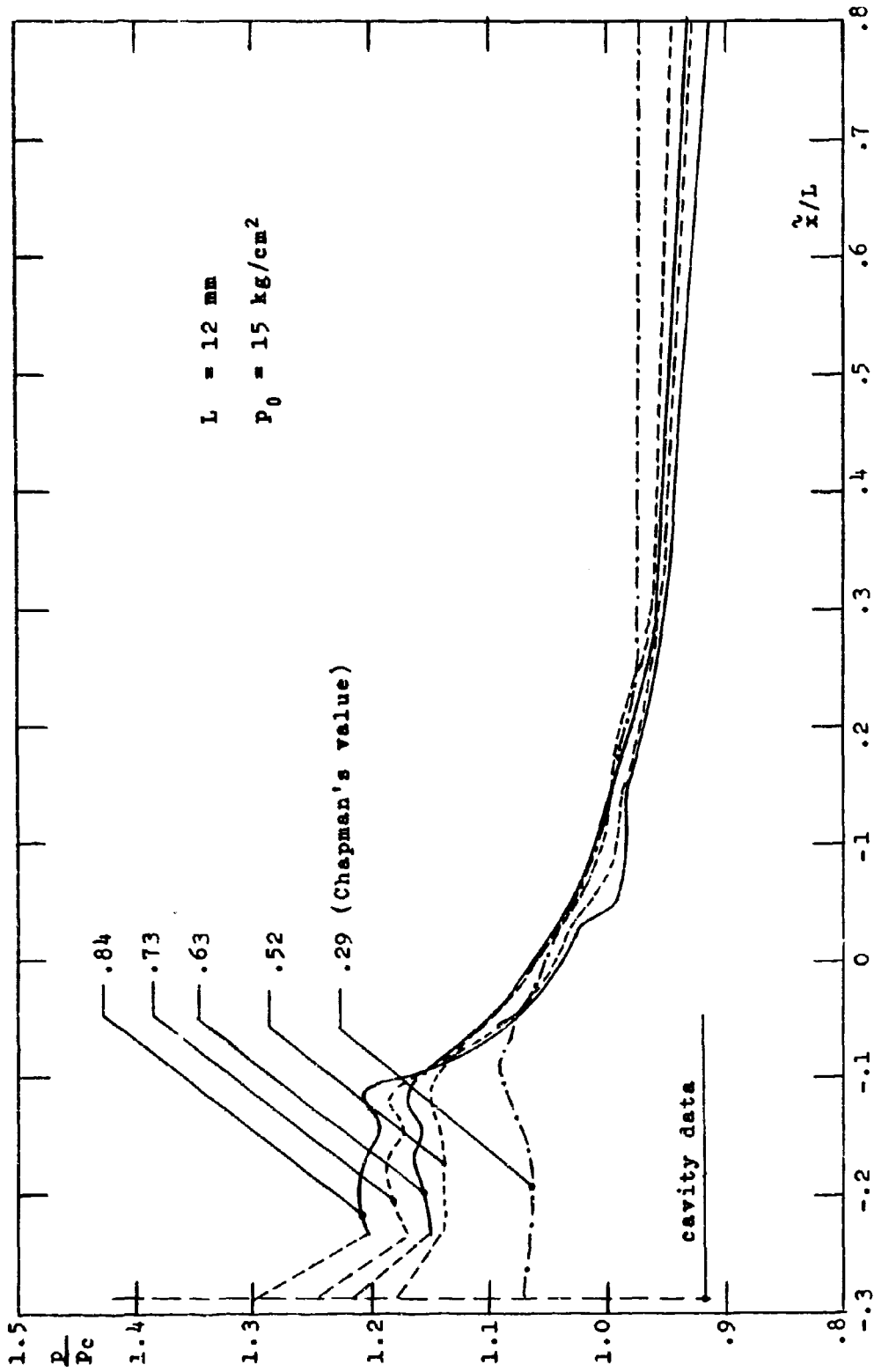


Figure 3. Effect of mass injection on pressure distribution (concluded)

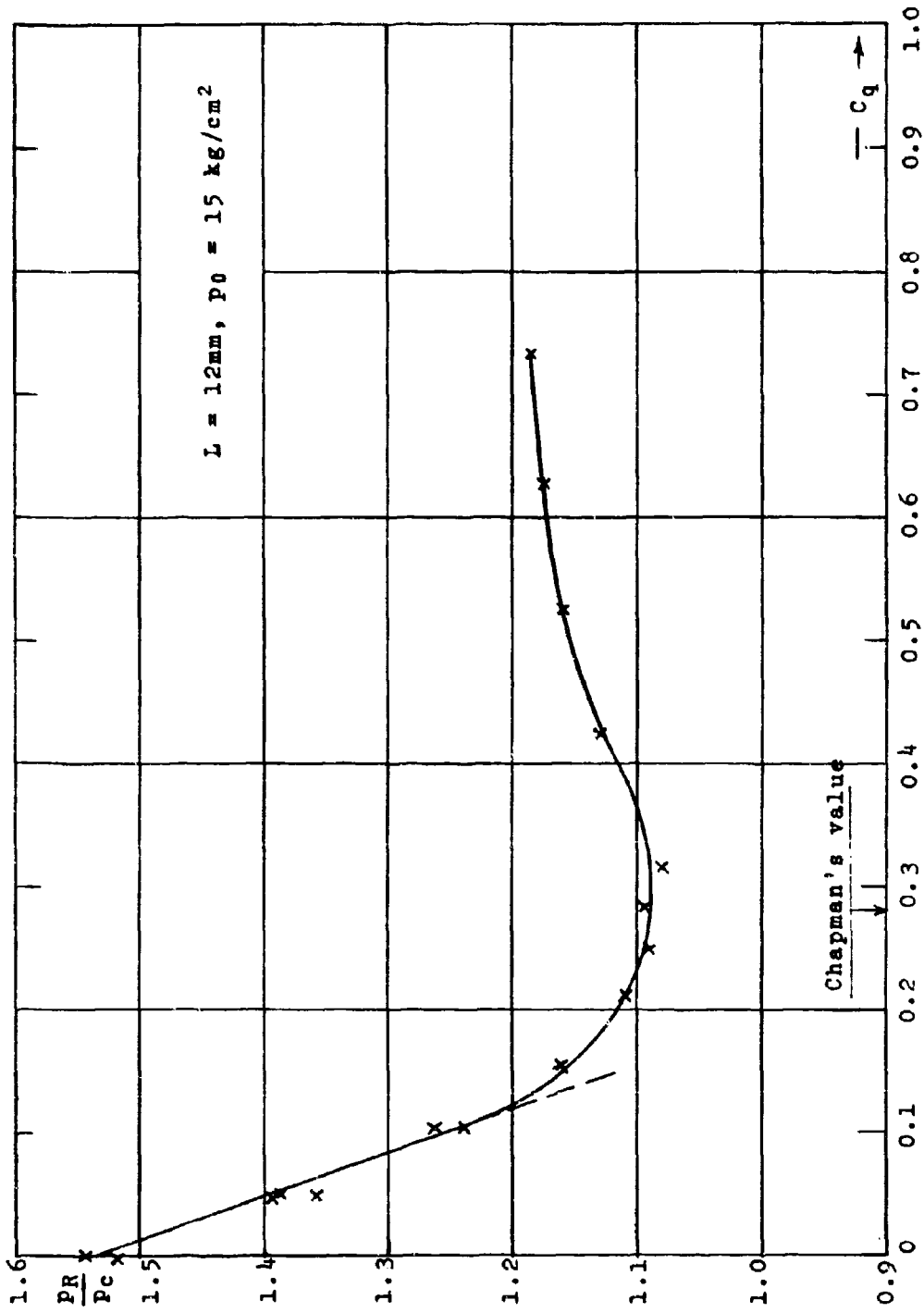
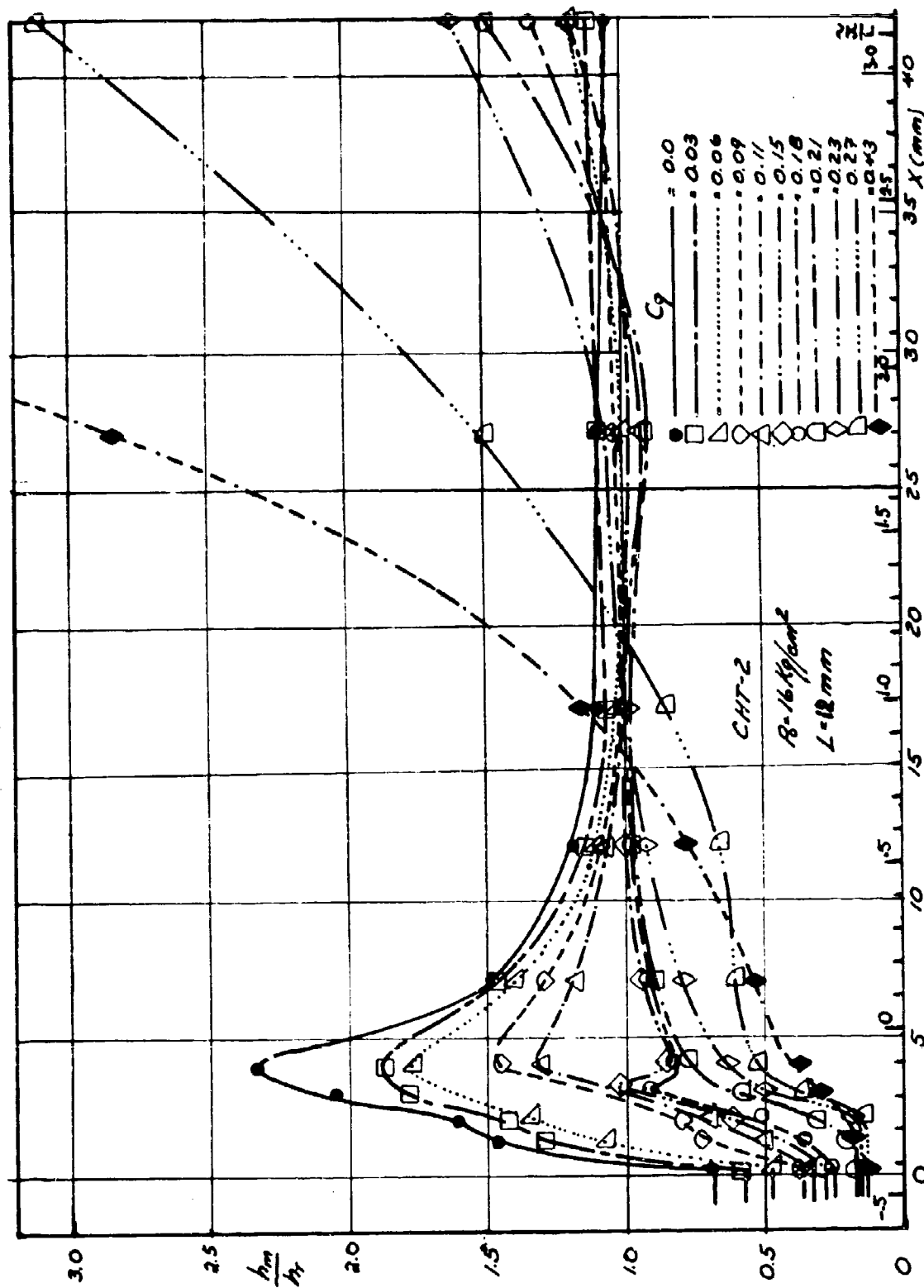


Figure 4. Peak pressure ratio as a function of mass injection rate



EFFECT OF MASS INJECTION ON HEAT TRANSFER DISTRIBUTION
OVER A CONE CAVITY MODEL AT $M=5.41$ ON CHT-2

FIGURE 5

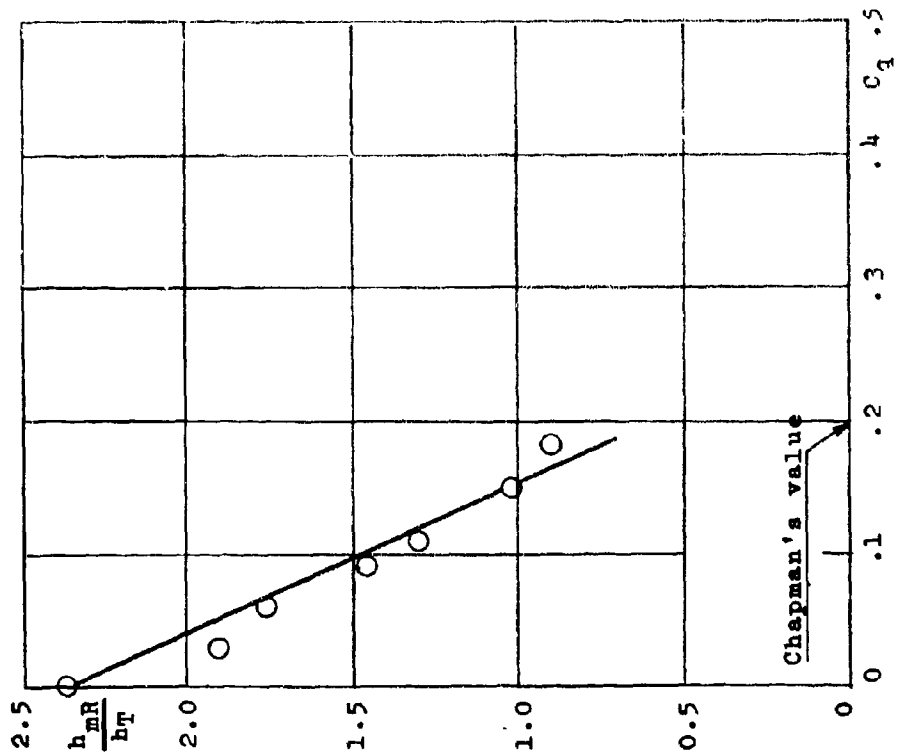


Figure 7. Maximum heat transfer ratio

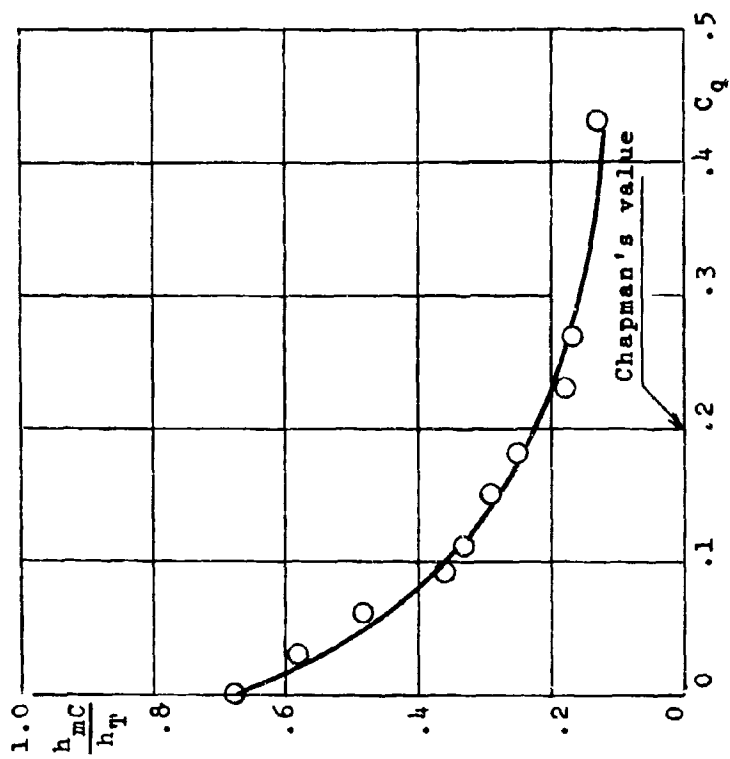


Figure 6. Minimum heat transfer ratio

UNCLASSIFIED

Security Classification

DOCUMENT CONTROL DATA - R & D		
<i>(Security classification of title, body of abstract and indexing annotation must be entered when the overall report is classified)</i>		
1. ORIGINATING ACTIVITY (Corporate Author)		2a. REPORT SECURITY CLASSIFICATION
von Karman Institute for Fluid Dynamics High-speed laboratory		unclassified
		2b. GROUP
3. REPORT TITLE		
LAMINAR SEPARATION IN HYPERSONIC FLOW		
4. DESCRIPTIVE NOTES (Type of report and inclusive dates)		
Scientific. Final. 1-10-1966 30-9-1967		
5. AUTHOR(S) (First name, middle initial, last name)		
Jean J. GINOUX		
6. REPORT DATE	7a. TOTAL NO OF PAGES	7b. NO OF REFS
30-11-1967	19	9
8a. CONTRACT OR GRANT NO.	8b. ORIGINATOR'S REPORT NUMBER(S)	
AF EOAR 67-09	VKI-CR-67-6I-I-1	
6. PROJECT NO 9781-02		
c. DOD element : 61445014	9b. OTHER REPORT NO(S) (Any other numbers that may be assigned this report) AFOSR 68-0231	
d. DOD Subelement : 681307	VKI-CR 67-29-1-1-67-186	
10. DISTRIBUTION STATEMENT		
This document has been approved for public release and sale ; its distribution is unlimited.		
11. SUPPLEMENTARY NOTES	12. SPONSORING MILITARY ACTIVITY	
TECH, OTHER	Air Force Office of Scientific Research (SREM). 1400 Wilson Blvd. Arlington - Va. 22209	
13. ABSTRACT		
An experimental investigation of the laminar flow over a cone-cavity model with a rounded reattachment shoulder at zero angle of attack was conducted at M=5.4. For mass injection into the cavity at rates up to eight-tenths the boundary layer mass flow at separation, the pressure and heat transfer distributions along the surface were obtained, with emphasis on the reattachment zone. A simple empirical correlation was established between reattachment pressure and heat transfer peaks as a function of injection rate.		

DD FORM 1473
1 NOV 65

UNCLASSIFIED
Security Classification

UNCLASSIFIED
Security Classification

14 KEY WORDS	LINK A		LINK B		LINK C	
	ROLE	WT	ROLE	WT	ROLE	WT
Laminar flow Separation Hypersonic speeds Mass injection Static pressure Heat transfer Cone-cavity models Zero angle of attack						

UNCLASSIFIED
Security Classification